HEFAT2012
9th International Conference on Heat Transfer, Fluid Mechanics and Thermodynamics
16 – 18 July 2012
Malta

LINEAR STABITLITY ANALYSIS OF A SUPERCRITICAL LOOP

T'Joen, C.[1]*, Rohde, M.[2] and De Paepe, M.[1]
*Author for correspondence
[1]Department of Flow, Heat and Combustion Mechanics
Ghent University-UGent
Sint-Pietersnieuwstraat 41, 9000 Gent
Belgium
E-mail: christophe.tjoen@ugent.be

[2]Department of Radiation, Radionuclides and Reactors
Delft University of Technology
The Netherlands

ABSTRACT

Because of their unique properties, supercritical fluids are becoming increasingly popular for industrial applications. These fluids behave liquid like at low temperatures and gas like at higher temperatures, with a smooth transition in between. This makes them very suited as a solvent for chemical extraction and separation processes. Another important use is as a power fluid. Modern fossil fuel fired power plants all operate using supercritical water, and on a smaller power scale they are considered for organic rankine cycles and refrigeration.

As they heat up, the density of a supercritical fluid changes shows a very sharp drop for temperatures close to the critical point. This large density difference can be used as the driving force to circulate the fluid in a loop, rather than using a pump. This idea is similar to natural circulation boiling loops, but the density difference is larger. It adds a layer of inherent safety to a design, as active components such as pumps are no longer required; but also adds an additional complexity: flow instabilities. It is well known from natural circulation boiling systems, that these loops can become unstable under certain conditions (e.g. high power and low flow rate).

In this study, a simple supercritical loop is studied to determine the neutral stability boundary. This is done through linear stability analysis: the set of one-dimensional governing equations is first linearised and then the eigenvalues are determined. These describe the response, indicating if it is stable or not. The results indicate that there is a clear unstable area, which can be linked to different types of instabilities.

INTRODUCTION

It is well known from thermodynamics that increasing the heater outlet temperature in a thermal cycle will result in a higher thermal efficiency (Carnots law). This has driven the development of power stations worldwide, pushing the turbine inlet temperature and pressure higher, starting from about 500°C, 180 bar during the 70s to current units operating at 300 bar, 600-650°C. New units, so called 'ultrasupercritical power stations' are in development to operate at 360 bar with a turbine inlet temperature of 700°C and higher. These are expected to become operational past 2020. Modern coal fired power stations have a thermal efficiency of up to 45% and if a combined cycle is used the most advanced units just fall short of 60%. Compared to these numbers, the thermal efficiency of the nuclear reactors currently in operation (33-34%) and even the more advanced units under construction (Gen III+, EPR is rated at 37-38%) is low. This is due to the lower pressure and temperature used in these cycles (150 bar, 315°C for a PWR) which is related to the stringent safety criteria, neutronics, thermohydraulic interactions and material properties. To increase the thermal efficiency, a light water cycle based on supercritical water (SCWR, SuperCritical Water Reactor) has been proposed as part of the GenIV platform. This cycle would operate at 25 MPa, with an inlet and exit temperature of 280 °C and 500 °C respectively and an estimated efficiency between 42 and 45%. During the past decades a number of SCWR designs have finalized, including a European one [1]. Other GenIV nuclear reactor designs are considering a supercritical CO_2 Brayton cycle as power cycle. On a smaller power scale there has been a lot of interest to use supercritical CO_2 as a natural refrigerant instead of Freon based hydrocarbons in compression cooling cycles as part of the ongoing struggle to reduce greenhouse gas emissions (see e.g. Kim et al. [2]). Supercritical organic fluids are also considered for ORC cycles aimed at low temperature energy recovery, Schuster et al. [3].

NOMENCLATURE

A	[m²]	Tube cross sectional area
C_j	[-]	local friction coefficient
C_p	[J/kgK]	Specific heat capacity
Dh	[m]	hydraulic diameter
f	[-]	friction factor
g	[m/s²]	gravitational acceleration
G	[kg/m²s]	Mass flux
h	[J/kg]	enthalpy
k	[W/mK]	Thermal conductivity
L	[m]	heater length
p	[Pa]	pressure
P	[Pa]	dynamic pressure
P_h	[m]	heated perimeter
Q	[W]	Heat input
$q"$	[W/m²]	surface heat flux
Re	[-]	Reynolds number
t	[s]	time

Greek characters

θ	[rad]	angle relative to horizontal
μ	[Pas]	dynamic viscosity
ρ	[kg/m³]	density
υ	[m³/kg]	specific volume

subscripts

in	inlet
pc	pseudocritical

It is well known that supercritical fluids experience a strong change in properties as they heat up or cool down. This is illustrated in This graph shows the scaled transport properties of water at 25 MPa. All properties are scaled to the value at 200°C apart from the specific heat capacity, which is scaled to its maximum value. The specific heat capacity for supercritical fluids has a very typical behaviour, showing a strong localised maximum as a function of temperature. The temperature which corresponds to the maximum is referred to as the pseudo-critical temperature. For pressures close to the critical pressure (just above), the peak becomes sharper and more pronounced.

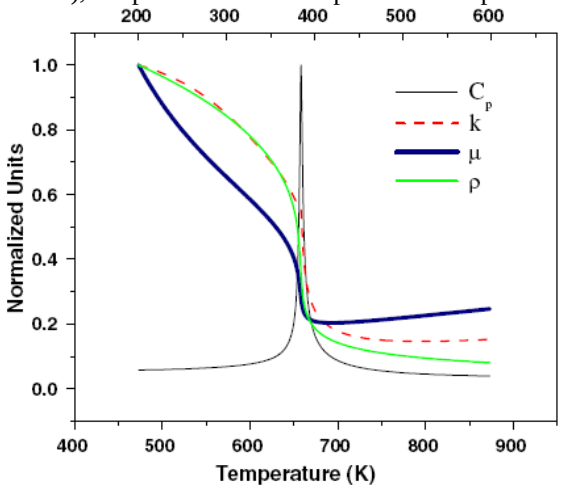

Figure 1 Illustration of the transport properties (density, thermal conductivity, dynamic viscosity and specific heat capacity) for water at 25 MPa for varying temperature.

The behaviour shown in Figure 1 is common to all supercritical fluids. In fact, Ambrosini et al. [4] and Ambrosini [5] compared the non dimensional fluid properties of water, CO_2, ammonia and Freon R23. They showed that if the pseudocritical properties are used as reference values, the curves of the different fluids match very well. These sharp fluid property changes have a strong effect on the thermo-hydraulics. Due to the strong density gradients near to the heated or cooled walls, the fluid behaviour becomes very complex due to combined effects of buoyancy and flow acceleration/ deceleration. A large number of experimental campaigns have been performed studying supercritical heat transfer, resulting in a large set of correlations, see e.g. [6]-[7] for reviews. However, when compared to experimental data, these correlations often show a very large scatter. New models and heat transfer deterioration criteria are being developed which include new non-dimensional numbers to quantify the buoyancy and flow acceleration (e.g. [8]).

Considering the large density difference that a supercritical fluid undergoes as it heats up, natural circulation could be considered as the driving force of the system. This removes the need for active components such as pumps, making the system more safe. This idea is currently being explored for the SCWR [9]. Natural circulation loops can however become unstable under specific operational conditions (e.g. high power and low flow rate). Bouré et al. [10] presented a classification of the different types of instabilities and an overview of earlier work. A static instability (flow excursion, the so called Ledinegg instability) can be described using only the steady-state equations. For this type of instability, a small change in the flow conditions will result in a new steady-state significantly different from the original one. For dynamic instabilities, such as density wave oscillations or DWO, the steady-state equations are not sufficient to predict the system behavior, not even the threshold of instability. In such a situation, multiple competing solutions exist for the governing equations, and the system cannot settle down into anyone of them permanently. The system will move from one solution to the other, driven by feedback mechanisms. March-Leuba and Rey [11] presented a detailed explanation of the DWO and the feedback mechanisms, which is driven by the interaction of inertia and friction for the thermo-hydraulic modes.

Most published results on the stability of supercritical flows are numerical and they consider either a forced single pass system ([4]-[5], [12]) or an idealized loop geometry (e.g. [13]-[15]). These results were obtained using different numerical codes which apply various techniques to study the stability (such as an eigenvalue analysis, transient simulations or root finding of characteristic polynomials). Experimental data on natural circulation supercritical loops is rare in open literature, and as such, validation of these codes is difficult. For a single-pass, Ambrosini and Sharabi [4] compared three different methods to determine the stability boundary. Based on the good agreement between these methods and their diversity, they concluded their results were physically correct.

The goal of this study is to examine the stability boundary of a naturally circulating supercritical loop experimentally. The used model will first be described and then validated by comparing results to previously published studies. The results will then be presented which indicate that different competing

instability modes (similar to boiling systems) define the stability plane of a simple natural circulation loop.

MODEL DESCRIPTION

The considered system is a very simple thermosyphon. It is shown in Figure 2. It consists of a horizontal heater (bottom) and cooler (top) with a length of 0.5m. These are connected by an adiabatic riser / downcomer with a length of 2m. The tube diameter is uniform over the loop: 0.006m. To describe the bends with a local pressure drop, these are modelled as segments with a length of 0.05 m, so the total flow length is 5.2m. This loop is similar to those previously studied by e.g. Jain and Uddin [13]. The dimensions are inspired by the experimental facility DeLight that has been constructed at the Delft University of Technology to study the coupled thermo-hydraulic – neutronic instability of a SCWR, [9]. This loop operates using Freon R23, and this fluid is then also considered for these simulations, operating at a pressure of 5.7 MPa. A previous study has shown that this fluid is a good scaling fluid for supercritical water, Rohde et al. [16]. The non-dimensional fluid properties of both fluids agree well, with a maximum deviation of 8% for the density far away from the pseudo-critical point.

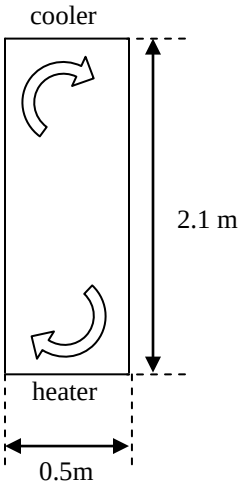

Figure 2 Schematic of the considered loop

To describe the thermo-hydraulic behavior of this system, the 1-D transport equations are used. The code thus calculates cross sectional averaged properties. The equation set consists of the time dependent conservation of mass, momentum and energy, expressed as a function of the mass flux (G), pressure (p) and enthalpy (h). These are equations (1)-(3). To close this system of equations an equation of state is needed, linking the fluid density to the variables. Because the density varies much less with pressure than with enthalpy, and the pressure change of the system is small (0.12 MPa compared to the system pressure of 5.7 MPa), the density is described as a function of enthalpy only. In the equation for the momentum conservation, the Darcy-Weisbach friction factor is used in combination with local C_j friction values for the bends (as indicated by the delta function). θ indicates the angle relative to the horizontal axis, which is set to 0° in this study.

$$\frac{\partial \rho}{\partial t} + \frac{\partial G}{\partial z} = 0 \tag{1}$$

$$\frac{\partial G}{\partial t} + \frac{\partial}{\partial z}\left(\frac{G^2}{\rho}\right) = -\frac{\partial p}{\partial z} - g\rho\sin\theta - \frac{G^2}{2\rho}\left[\frac{f}{D_h} + C_j\delta\left(z - z_j\right)\right] \tag{2}$$

$$\frac{\partial \rho h}{\partial t} + \frac{\partial (Gh)}{\partial z} = \frac{q'' P_h}{A} \tag{3}$$

To describe the stability behavior of a supercritical system non-dimensional numbers have been derived. These have been mostly inspired by the earlier work done on boiling systems, seeking to extend the concept of the subcooling number and the phase change number into the supercritical range, as can be read in Ortega Gómez et al. [12] and Ambrosini and Sharabi [4]. Ambrosini [17] showed that the stability of a single heated pipe with a supercritical fluid is similar to that of a boiling channel, experiencing both Ledinegg instabilities and DWO. Based on his analysis, he defined the 'sub pseudocritical number' N_{SUBPC} and the 'trans pseudocritical number' N_{TPC} to define the stability plane. In their scaling analysis, Rohde et al. [16] derived two similar non-dimensional properties, by using the pseudo critical values as reference. These are the so cooled subcooling number N_{SUB}, Eq. (4) and the phase change number NPCH, Eq. (5). In the remainder of this work these will be used. The considered pseudocritical enthalpy for Freon R23 at 5.7 MPa is 288.33 kJ/kg.

$$N_{SUB} = \frac{\left(h_{pc} - h_{in}\right)}{h_{pc}} \tag{4}$$

$$N_{PCH} = \frac{q''\cdot P_h \cdot L}{G \cdot A \cdot h_{pc}} \tag{5}$$

NUMERICAL IMPLEMENTATION

To simulate the system, a numerical model is required. This model was built in the Comsol© software package. This is a finite element analysis software environment for the modelling and simulation of so called 'multi-physics' problems where different phenomena interact. Standard modules exist to add e.g. 1-D flow and heat transfer problems, but in this study the basic 1-D PDE coefficient mode was used whereby the equations are added to the model, and Comsol© acts as the solver. To fit in the predefined Comsol© PDE coefficient structure, the equations had to be rewritten in a slightly different form from Eqs. (1-3) to Eqs. (6-8). Important to note is that to this end the static pressure p was transformed into the dynamic pressure P in the momentum equation (Eq. (9)), to result in a form with only one spatial partial derivative. As such the solved variables are now enthalpy h, dynamic pressure P

and mass flux *G*. The derivative of the specific volume with regards to the enthalpy can be rewritten through Eq. (10) as a function of the density derivative. Ortega Gómez et al. [12] previously used the same set of equations in Comsol© to study the stability of a single heated channel. By making an initial guess for the mass flux, e.g. G = 1500 kg/m²s, the enthalpy profile can be determined from the heat balance. The final solution was found to be insensitive to the initial guess for G, but using a higher value resulted in a faster convergence. The enthalpy values can then be used to compute the substance properties and then solve the momentum equation. By then iterating until the pressure difference over the loop equals zero, the steady solution is found.

$$\frac{\partial h}{\partial t} = \upsilon^2 \frac{\partial G}{\partial z}\left(\frac{\partial \upsilon}{\partial h}\right)_p^{-1} \tag{6}$$

$$\frac{\partial G}{\partial t} = -\frac{\partial P}{\partial z} - \frac{g}{\upsilon}\sin\theta - \frac{G^2\upsilon}{2}\left[\frac{f}{D_h} + C_j\delta\left(z - z_j\right)\right] \tag{7}$$

$$\frac{\partial h}{\partial t} + G\upsilon\frac{\partial h}{\partial z} = \frac{q'' P_h \upsilon}{A} \tag{8}$$

$$p + G^2\upsilon = P \tag{9}$$

$$\left(\frac{\partial \upsilon}{\partial h}\right)_p = -\frac{1}{\rho^2}\frac{\partial \rho}{\partial h} \tag{10}$$

To define the substance properties, the NIST REFPROP (v7) database was used. The density and viscosity at 5.7 MPa were determined as a function of the enthalpy over a wide range of temperatures (-80°C to 500 °C). Ortega Gómez et al. [12] previously studied the effect of various approximations to define supercritical fluid properties (e.g. a two or three region model]), and they found that these approximations have a significant impact on the results. Therefore great care was taken to ensure the fluid properties are well defined by using a series of splines. These are based on data points which are carefully spread over the selected temperature range, concentrating more points near the pseudocritical point to capture the steep change. A comparison between the density and viscosity data from the NIST REFPROP data between -80 °C and 500 °C evaluated every 0.1 °C shows a maximum difference of 0.8% compared to the spline interpolations. In particular care had to be taken to define $\frac{\partial \rho}{\partial h}$. To determine this property, the central difference approximation was used on a fine mesh of tabulated density and enthalpy values. It is important that this mesh is sufficiently fine, as determining the derivative based on a coarse mesh will result in a very different curve shape of the derivative as a function of the enthalpy, as shown in T'Joen et al. [18] .

This set of equations was programmed in combination with the geometry and the boundary conditions. The domain consists of 8 zones, the heater, riser, cooler, downcomer and four bends. In the heater and cooler a uniform heat flux are imposed, for all other zones the heat flux is zero. The local friction coefficient C of the bends was set to 0.5. In the bend zones the wall friction and gravity are neglected, so these sections only account for the local pressure drop. To describe the wall friction in all zones apart from the bends, the Haaland relationship [19] was used. This is an approximation of the more exact Colebrook-White equation, valid for Re > 20000. It was verified that within the considered power range, the Reynolds number did not go below this value. The wall roughness was set to 4e-7. This value was also used in the previous study of a single heated channel ([18]) and is based on measurements of the wall roughness of the stainless steel tubes used in the DeLight setup. The inlet enthalpy and inlet pressure are imposed at the start of the heater. To ensure the system behaves as a natural circulation loop, the static pressure difference between the two ends of the domain is set to zero. This was done by specifying 'periodic boundary conditions' for the two end points.

MODEL VERIFICATION

Comsol© makes use of 'shape functions' to compute the solution. Different types of shape functions are available (Lagrange, Hermite) of which the order can be set as well, ranging from 1st to 5th order. In this study Lagrange elements were used of order 5, similar to what was used by Ortega Gomez et al. [12]. Reducing the order of the elements down to two or changing the type to Hermite had no effect on the final solutions (both the predicted steady state and the predicted stability line were the same). A grid independence study was performed. It was found that the predicted steady state mass flux and the stability line are very insensitive to the number of elements used in the simulations: the largest difference in N_{PCH} values between a simulation with 74 cells and the reference case (208 cells) was less than 0.25%, as illustrated in Figure7 and Table 1. A grid distribution of 208 cells was selected with 5 cells in each orifice zone. This grid was used for the presented simulations.

Table 1: Illustration of the grid independence of the steady state values

Hin	Q	74 cells	104 cells	208 cells
181860	500	0,014896	0,014896	0,014896
181860	2250	0,02639	0,02639	0,02639
181860	5000	0,027389	0,027389	0,027389
213950	500	0,015719	0,015719	0,015719
213950	2250	0,026019	0,026019	0,026019
213950	5000	0,020908	0,020908	0,020908
263740	500	0,01558	0,01558	0,01558
263740	2250	0,017847	0,017847	0,017847
263740	5000	0,013221	0,013221	0,013221

To determine the steady state solution a numerical solver routine is needed. Different solvers were compared, and the UMFPACK routine was finally selected. The convergence

criterion was set to 1e-8, and most cases converged within 20 iterations. Setting this value lower had no effect on the mass flux prediction. To determine the stability behavior of the system, the eigenvalue approach was selected. Comsol© offers the option to linearize the system around the computed steady state solution, and then to determine the eigenvalues of this new set of equations. The sign of the eigenvalue with the largest real part then indicates if the system is stable or not. The same solver routine was used (UMFPACK) during the eigenvalue computations and a set of 150 eigenvalues were determined and sorted. A careful analysis was performed to determine the number of eigenvalues that are required to accurately determine the stability boundary. Increasing the number, in some cases resulted in a new set of unstable eigenvalues appearing with a higher frequency. This is due to the sorting algorithm part of Comsol© which sorts the eigenvalues based on the distance to the origin (or a selected value). No difference was found in the stability boundary predicted by using 100, 150 or 200 eigenvalues as output. So 150 eigenvalues was used to perform the computations. Furthermore, it was found that a number of the eigenvalues that appear in the solution list are in fact numerical artifacts. These typically have very high imaginary components, and when one plots the corresponding eigenfunction, a very noisy result can be seen. Refining the grid only has a small to negligible effect on the other eigenvalues, but these eigenvalues with a very high imaginary component shifted strongly to even higher frequencies. This led us to conclude that these solutions are not physical and they were thus filtered out.

MODEL VALIDATION

In a previous study ([18]) the same set of equations and code were used to study the stability of a single heated channel. The code was validated by comparing steady state data and the stability line to data of Ambrosini and Sharabi [4]. Very good agreement was shown. To validate this loop code, a similar approach is used. The loop presented by Chatoorgoon [20] with supercritical water and by Jain and Uddin [13] with supercritical CO2 were considered as validation cases. In Figure 3 a comparison is presented between the steady state results of Chatoorgoon [20] and the predictions using the Comsol code. The fluid properties of water were obtained from the NIST database, and these splines are described in more detail in [18]. Chatoorgoon used a set of three fixed friction constants, depending on the location in the loop, thus removing the impact of the Reynolds number in the computations. As can be seen, there is a very good agreement. Chatoorgoon [20] also presented stability data in his paper, but these were later shown to be not fully converged by Jain and Uddin.

In Figure 4 a comparison is presented between the steady state data of Jain and Uddin [13] and the Comsol code. The splines to describe CO_2 fluid properties were again based on the NIST database. They used a different frictional relationship (Mc Adams) instead of the Haaland equation. As can be seen, just as for the data of Chatoorgoon, the agreement is very well. Jain and Uddin also presented stability data for a number of cases. One included the impact of the inlet temperature. Only 5 data points were presented listing the power required for their loop to become unstable at a given inlet temperature. To determine the corresponding N_{PCH} number, the mass flow rate is required, which was determined by running the simulation for these conditions. The results are shown in Figure 5. As can be seen, there is a good agreement between the data and predictions using the Comsol code.

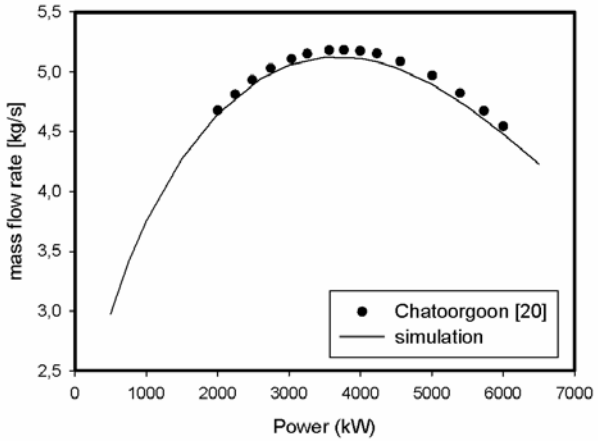

Figure 3 Comparison of the steady state results of Chatoorgoon [20] to the predictions using the Comsol code

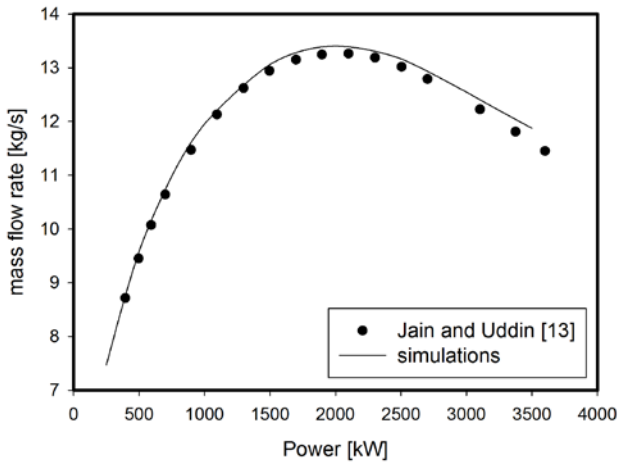

Figure 4 Comparison of the steady state results of Jain and Uddin [13] to the predictions using the Comsol code

RESULTS

The proposed validated model was used to study the stability of the natural circulation loop shown in Figure 2. First, the steady state results will be presented. Figure 6 shows the steady state predicted mass flow rate for different inlet temperatures. The data series show the typical 'maximum' behavior inherent of natural circulation loops. Increasing the power at low power ranges results in an increase of the driving force in the loop and a moderate increase of the friction (low fluid velocity). This combined results in a higher flow rate. At higher power however, increasing the power results in a small increase of the driving force, but a substantial increase of the frictional pressure drop. This results in a net decrease of the mass flow rate. Lowering the inlet temperature raises the

density in the loop, which provides additional driving force. So the mass flow rate that can be obtained is higher. However, the driving force is related to the density difference between the hot and the cold leg. As can be seen in Figure 1, the density curve has an elongated S shape, indicating that for low temperatures (fluid like) and high temperatures (gas like) the density is less affected by the temperature than in between these zones. Lowering the inlet temperature, shifts the density more into the 'liquid like' plateau of the density curve, and as a result more power is needed to generate a substantial difference between the hot and cold leg. This explains why in Figure 6 at lower power the higher inlet temperatures provide a slightly higher mass flow rate.

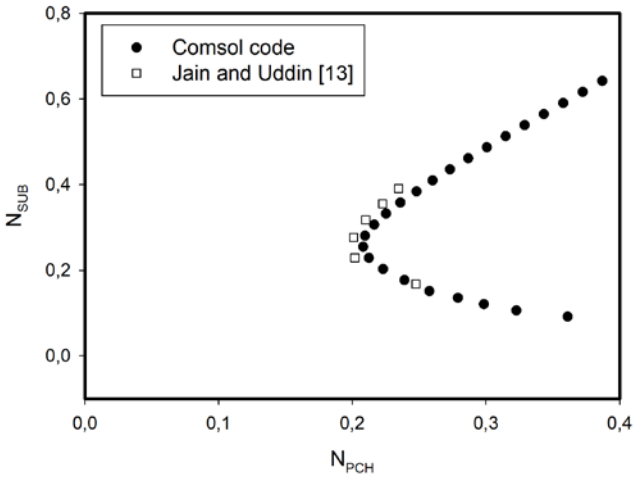

Figure 5 Comparison of the stability data of Jain and Uddin [13] to the predictions using the Comsol code

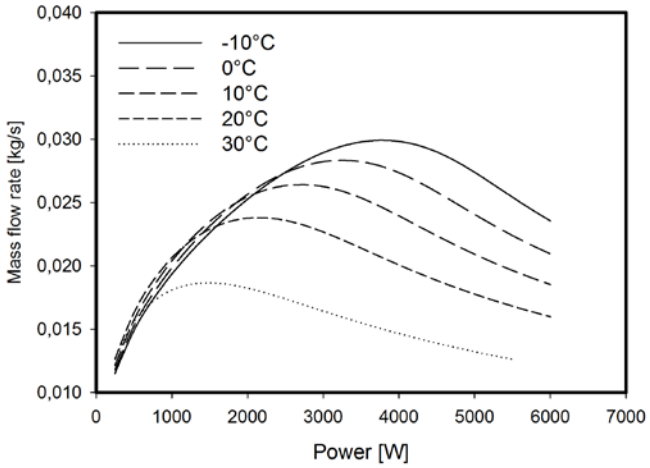

Figure 6 Steady state predicted mass flow rate for varying inlet temperature

The stability boundary of the considered loop can be seen in Figure 7. Results are shown for two grid sizes: 0.025m and 0.05m. As can be seen, these curves correspond perfectly. The red dashed area at the right lower part of the graph cannot be reached, because of the limiting temperatures of the substance property splines. The stability curve has a similar 'curved L' shape as that of a single heated channel. However, as an additional feature, there is a second 'bump' which is also 'cut off' before dropping off towards N_{SUB} = 0. This behaviour is qualitatively similar to that of a boiling water system, as shown in Figure 8. For a boiling system it is well known that there are 2 characteristic types of density wave oscillations, the type I (low void fraction) and the type II (high power). This results in a 'bump' in the stability plane. The results in Figure 7 show a similar pattern, plot out using the equivalent non-dimensional numbers for a boiling system: the subcooling number (now defined using h_{sat} instead of h_{pc} as reference value) and the Zuber number, [4]. There are some remarkable differences as well. Firstly, a boiling system has two boundaries it can never cross: the diagonal of the stability plane and the x-axis. Operating to the left of the diagonal results in no boiling occurring, and thus there is no density gradient to trigger the oscillations; operating below the x-axis would indicate that only vapour enters the heater, which also results in very small density gradients. For the supercritical system, both boundaries can be crossed, which is due to the continuous profile of the density vs. enthalpy (as shown in Figure 1). The diagonal (indicated by the dashed line in Figure 7) is crossed over at a low N_{SUB} and the boundary then moves slowly away from the diagonal at higher N_{SUB} values. That the boundary is crossed makes sense, as the density changes already a lot even before reaching the pseudo-critical point. There is thus an ample gradient already present to trigger the oscillations. The x-axis is only just crossed at the highest reachable N_{PCH} for this study.

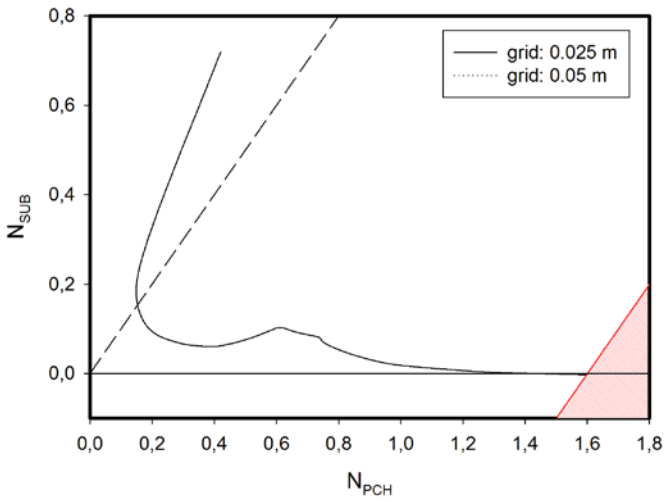

Figure 7 Stability boundary for two grid sizes.

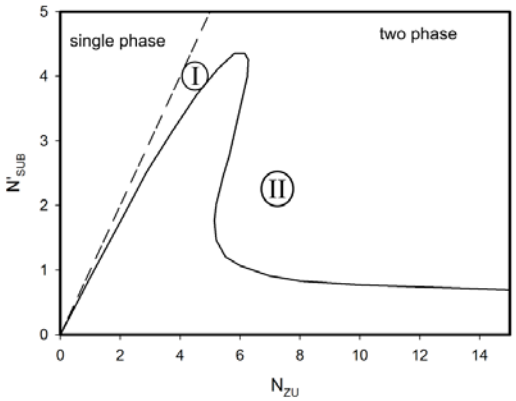

Figure 8 Schematic illustration of the stability plane of a boiling water system, [21]

The behaviour shown in Figure 7 has so far never been demonstrated in open literature. As can be seen in Figure 5, the data points of Jain and Uddin are located on the first branch of the stability line, near to the bend. Sharma et al. [14] predicted a similar left branch of their stability boundary, but their solution indicates a similar branch at higher power, resulting in a 'parabolic' shape of the unstable area. This would suggest that for very high power, the system in fact is stable, which feels counter-intuitive, based on the results of the boiling systems. In a recent set experiments on the DeLight facility, the coupled neutronic – thermo-hydraulic instability of the system was explored, exploring the inner section of the 'bump' in the stability plane, [9]. The left boundary in the stability plane was found at a very comparable location as in this study. This suggests that this forms a fundamental mode of a supercritical loop. Ambrosini [17] previously also concluded that there are strong similarities between the instabilities of a single heated channel with a boiling fluid and with a supercritical fluid. This all suggests that the data shown in Figure 7 describes the general stability behaviour of a supercritical loop.

To better understand the behaviour shown in Figure 7, the oscillation frequency of the points located on the stability boundary are shown in Figure 9. This value is determined from the imaginary part of the eigenvalue. As shown there are 3 distinct groups or modes. Moving down along the left branch of the stability branch, the frequency is constant at 0.22 Hz, and close to the bend this starts to slowly increase. This increase is gradual and continues along the upward slope of the bump to a value of ~0.7 Hz. Then a jump in frequency appears, corresponding to the line which 'cuts' off the top of the bump. Along this line the frequencies slowly increase. Moving then onto the downward slope of the bump again results in a jump of the frequencies, which then gradually increase. The frequency of the first left branch is very similar to the value found in the experiments in the DeLight facility [18], 0.2 Hz, and those of Jain and Uddin [13], 0.15Hz. Such a sudden change in frequency also occurs in boiling systems when moving from type I to type II instabilities.

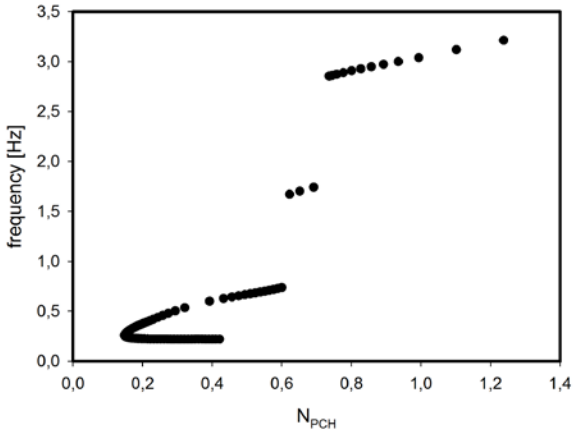

Figure 9 Oscillation frequency of the points located on the stability boundary

These jumps in the frequency were traced back to different sets of competing eigenvalue families which all cross from stable to unstable. And depending on the location on the stability line, one family crosses before the other and resulting in a frequency shift. This behaviour is further explored by plotting out these different families below. Figure 10 shows a contour plot of the real part of the low frequency mode. The stability line is indicated in white dashes. This line corresponds to the transition line (from positive to negative) of this mode along the bend, but then suddenly moves away. The 'transition line' for this mode continues to move upwards at higher power.

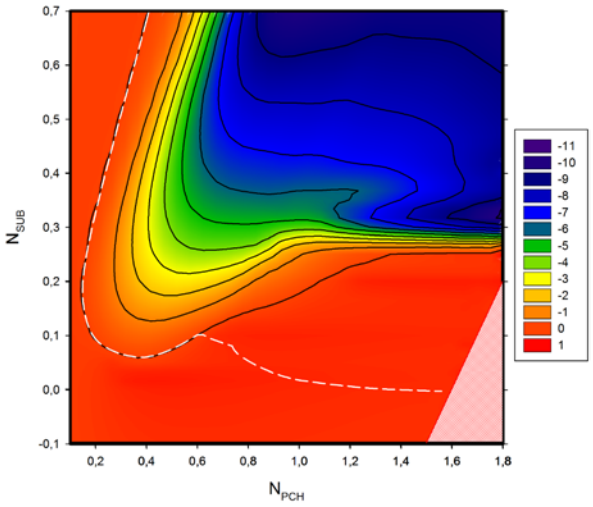

Figure 10 Contourplot of the real part of the dominant eigenvalue linked to the low frequency mode. Stability boundary in white dashes

The accompanying imaginary part is shown in Figure 11. The frequency trend of the left branch can clearly be seen again, first constant and then gradually increasing. Figure 11 reveals that higher power and high N_{SUB} values, a large number of dominant eigenvalues have a zero imaginary part (purple zone). This indicates an exponential behaviour, which is indicative of an excursive trend. Because this is linked to the

interaction of the pressure drop curve for varying flow rates, the pressure drop of the loop and of the heater on its own were further investigated. This is shown in Figure 12 for N_{SUB} 0.35 and Q = 1000W. The pressure drop over the loop forms a smooth curve and the intersection with the x-axis fixes the operating point. The core pressure drop curve shows a small dip, a local minimum. As the power is increased, the intensity of this local maximum increases. This is shown in Figure 13. At the same time, the operating point, indicated by the circle on the core pressure drop curves, slowly moves up the curve. At a certain moment, this operating point shifts onto the part of the curve with a negative slope. At this point the imaginary part falls back to zero and the behaviour becomes excursive. At higher power the operating point enters the region with a positive slope, and the imaginary part again becomes zero. This behaviour is thus linked to excursive behaviour of the horizontal heater. Ambrosini [4] had previously shown that a single horizontal heated channel with a supercritical fluid was indeed susceptible to Ledineg instabilities. In a loop, this affects the behaviour as well.

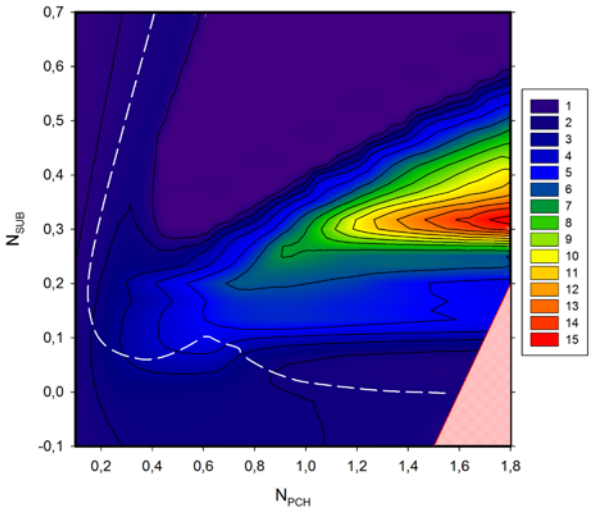

Figure 11 Contourplot of the imaginary part of the dominant eigenvalue linked to the low frequency mode. Stability boundary in white dashes

The contour plots of the real part of the dominant eigenvalue of the second and third mode are shown in Figure 14 and 15 respectively. The second mode forms a similar tilted L shape unstable region, but at higher power. The bend zone cuts off the tip of the bump in the stability plane. The third unstable mode is concentrated at higher power, forming the right side of the bump. For both these modes, the frequency plots have a very similar appearance as the real part.

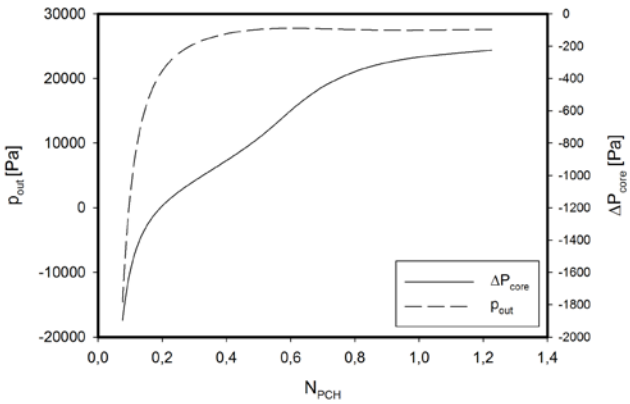

Figure 12 Loop and core pressure drop for varying mass flow rate at fixed power, N_{SUB} = 0.35, Q = 1000W

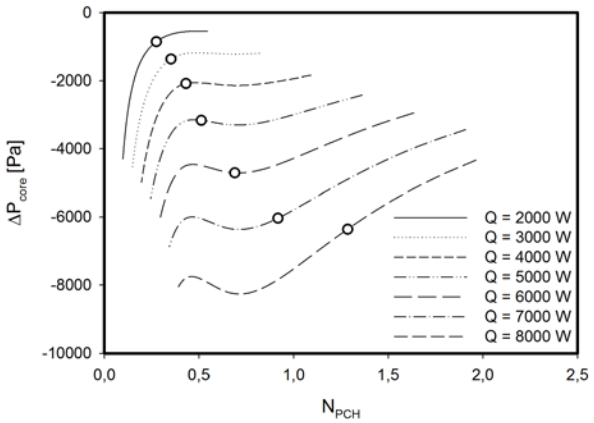

Figure 13 Core pressure drop for varying mass flow rate at different power levels, N_{SUB} = 0.35

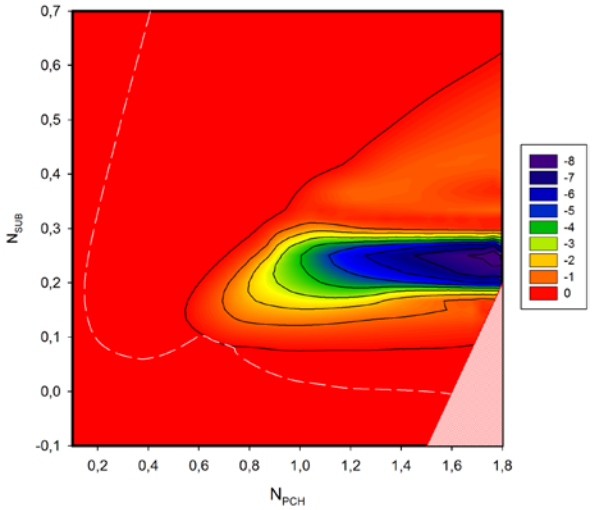

Figure 14 Contourplot of the real part of the dominant eigenvalue linked to the second frequency mode. Stability boundary in white dashes

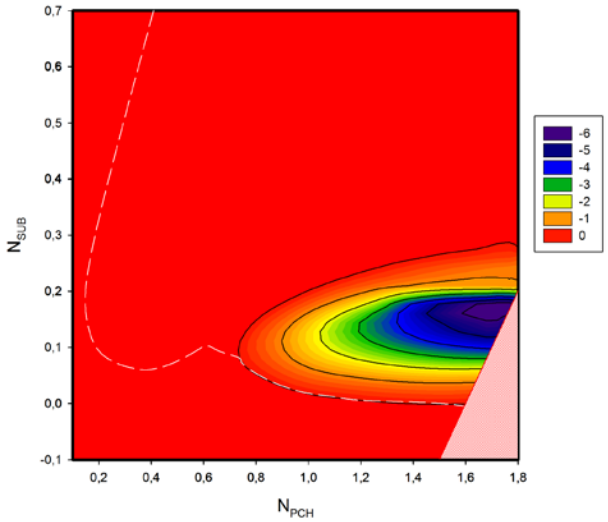

Figure 15 Contourplot of the real part of the dominant eigenvalue linked to the third frequency mode. Stability boundary in white dashes

The frequency value of the different modes provides information on the nature of the instability. The first mode relates to the mean loop circulation time. The slow increase in the frequency at the upward slope of the bump can be linked to the riser section. The other modes can be linked to the time it takes to travel through the heater only, similar as to boiling systems.

CONCLUSIONS

A numerical study was performed of the stability of a simple loop containing a supercritical fluid. Freon R23 was used at 57 bar as a scaling fluid for water, but the behaviour was described through non-dimensional numbers, making it universally valid. The 1D transport equations were solved using Comsol. The grid independence of the code was verified, and good agreement was shown with published numerical data. The results indicate parallels between the stability of a loop with a supercritical fluid and a loop with a boiling fluid. Different instability modes compete to form the stability plot. These were further explored. In particular for the first low frequency mode, linked to the loop circulation, showed the occurrence of eigenvalues with a zero imaginary part. This was related to the occurrence of a static instability in the heater section.

REFERENCES

[1] Fisher, K., Schulenberg, T., Laurien, E., Design of a supercritical water-cooled reactor with a three-pass core arrangement, *Nuclear Engineering and Design*, Vol. 239, 2009, pp. 800-812

[2] Kim, M.H., Pettersen, J., Bullard, C.W., Fundamental process and system design issues in CO2 vapor compression systems, *Progress in Energy and Combustion Science*, Vol. 30, 2003, pp. 119-174.

[3] Schuster A., Karellas S. And Aumann R., Efficiency Optimization Potential in Supercritical Organic Rankine Cycles, *Energy*, Vol. 35, 2010, pp. 1033-1039.

[4] Ambrosini, W., Sharabi, M., Dimensionless parameters in stability analysis of heated channels with fluids at supercritical pressure, *Nuclear Engineering and Design*, Vol. 238, pp. 1917-1929.

[5] Ambrosini, W., Discussion on the stability of heated channels with different fluids at supercritical pressures, *Nuclear Engineering and Design*, Vol. 239, 2009, pp. 2952-2963

[6] Pioro, I.L., Khartabil, H.F., Duffey, R., Heat transfer to supercritical fluids flowing in channels – empirical correlations (survey), *Nuclear Engineering and Design*, Vol. 230, 2004, pp. 69-91.

[7] Cheng, X., Schulenberg, T., Heat transfer at supercritical pressures – literature review and application to an HPLWR, FZKA6609, Forschungszentrum Karlsruhe GmBH, Karlsruhe, 2001, 47 pages

[8] McEligot, D.M., Jackson, J.D., "Deterioration" criteria for convective heat transfer in gas flow through non-circular ducts, *Nuclear Engineering and Design*, Vol. 232, 2004, pp. 327-333

[9] T'Joen, C., Rohde, M., Experimental study of the coupled thermo-hydraulic – neutronic stability of a natural circulation HPLWR, *Nuclear Engineering and Design*, Vol. 242, 2012, pp. 221-232.

[10] Bouré, J.A., Bergles, A.E., Tong, T.S., Review of two-phase flow instability, *Nuclear Engineering and Design*, Vol. 25, 1973, pp. 165-192

[11] March-Leuba, J., Rey, J.M., Coupled thermohydraulic-neutronic instabilities in boiling water nuclear reactors: a review of the state of the art, *Nuclear Engineering and Design*, Vol. 145, 1993, pp. 97-111

[12] Ortega Gómez, T., Class, A., Lahey Jr., R.L., Schulenberg, T., Stability analysis of a uniformly heated channel with supercritical water, Nuclear Engineering and Design, Vol. 238, 2008, pp. 1930-1939

[13] P.K. Jain, R. Uddin, Numerical analysis of supercritical flow instabilities in a natural circulation loop, *Nuclear Engineering and Design*, Vol. 238, 2008, pp. 1947-1957.

[14] Sharma, M., Pilkhwal, D.S., Vijayan, P.K., Saha, D., Sinha, R.K., Steady state and linear stability analysis of a supercritical water loop, *Nuclear Engineering and Design*, Vol. 240, 2010, pp. 588-598

[15] Jain, R., Corradini, M., A linear stability analysis for natural circulation loops under supercritical conditions, *Nuclear Technology*, Vol. 155, 2006, pp. 312-323

[16] Rohde, M., Marcel, C.P., T'Joen C., Class, A., Van der Hagen, T.H.J.J., Downscaling a supercritical water loop for experimental studies on system stability, *International Journal of Heat and Mass Transfer*, Vol. 54, 2011, pp. 65-74

[17] Ambrosini, W., On the analogies in the dynamic behavior of heated channels with boiling and supercritical fluids, *Nuclear Engineering and Design*, Vol. 237, 2007, pp. 1164-1174

[18] T'Joen, C., Gilli, L., Rohde, M., Sensitivity analysis of numerically determined linear stability boundaries of a supercritical heated channel, *Nuclear Engineering and Design*, Vol. 241, 2011, pp. 3879-3889

[19] Haaland, S.E., Simple and Explicit Formulas for the Friction Factor in Turbulent Flow, *Journal of Fluids Engineering*, Vol. 103, 1983, pp. 89–90.

[20] Chatoorgoon, V., Stability of supercritical fluid flow in a single channel natural convection loop, *International Journal of Heat and Mass Transfer*, Vol. 44, 2001, pp. 1963-1972

[21] Van Bragt, D.D.B., T.H.J.J. van der Hagen, 1998, Stability of natural circulation boiling water reactors: part II: parametric study of coupled neutronic-thermohydraulic instabilities, *Nuclear Technology*, Vol. 121, pp. 52-62